Structural, electronic, and optical properties of polyacetylene from a total-energy local-density molecular-cluster approach

L. Ye
Department of Physics and Astronomy and Materials Research Center, Northwestern University, Evanston, Illinois 60208
and Department of Physics, Fudan University, Shanghai, People's Republic of China

A. J. Freeman
Department of Physics and Astronomy and Materials Research Center, Northwestern University, Evanston, Illinois 60208
and Center for Materials Science, Los Alamos National Laboratory, Los Alamos, New Mexico 87545

D. E. Ellis
Department of Physics and Astronomy and Materials Research Center, Northwestern University, Evanston, Illinois 60208

B. Delley
Department of Physics and Astronomy and Materials Research Center, Northwestern University, Evanston, Illinois 60208
and Paul Scherrer Institute, c/o RCA Laboratories Ltd., Badenerstrasse 569, CH-8048 Zürich, Switzerland
(Received 10 February 1989; revised manuscript received 22 May 1989)

A self-consistent local-density total-energy molecular-cluster approach is used to study several fundamental structural, electronic and optical properties of *trans*- and *cis*-polyacetylene (PA). The use of extended basis sets in the linear combination of atomic orbitals (LCAO) representation and of accurate multipolar potential representations was found to be essential for obtaining accurate results. Chain clusters C_nH_{n+2} with increasing $n=8$, 12, 16, and 20 were investigated in order to assure convergence of physical quantities of interest. The ground-state density of states, energy gaps, and binding energies are obtained and compared with experimental results and results of other calculations. A gap of 1.68 eV is obtained for the *trans* case and 1.74 eV for *cis*. *trans*-PA is found to be a lower-energy state than *cis*-PA (by 0.1–0.2 eV per C_2H_2). Accompanying the Peierls transition from a metallic to semiconductor state, the dimerization energy is determined from optimized total-energy calculations on *trans*-PA to be about 0.02–0.03 eV/C_2H_2.

I. INTRODUCTION

Polyacetylene (PA) has attracted considerable attention from chemists and solid-state researchers in recent years and is looked upon as the prototype of a new class of materials with potential for novel technological applications. It is one of those quasi-one-dimensional (1D) polymers which can be a semiconductor or metal when suitably doped with donor or acceptor impurities. The possibility of soliton formation in lightly doped PA has stimulated the interest of both theorists and experimentalists,[1] and the promise of conducting polymers as fast-response, nonlinear-optical materials has also been emphasized recently.[2] The experimental literature is vast and cannot be reviewed here.

Several theoretical approaches have been put forward to discuss the electronic structure and properties of PA. Early on, the band structure of PA was studied by Grant and Batra[3] using semiempirical extended-Hückel-theory and tight-binding methods. They concluded that the gross electronic properties can be interpreted within the framework of an itinerant one-electron band structure. They compared the gaps and density of states (DOS) of three cases with varied C=C and C—C bond lengths, and noted the lifting of the degeneracy at the Fermi level as bond alternation occurs. A Hartree-Fock tight-binding linear combination of atomic orbitals (LCAO) study on *trans*- and *cis*-PA isomerism carried out by Karpfen and Holler[4] appeared to indicate that the trans configuration is the most stable structure of PA. Kasowski *et al.*[5] calculated the energy bands of pure and doped *trans*-PA with an extended muffin-tin-orbitals (EMTO) procedure and discussed the effect of heavy doping on the conducting properties. Grant and Batra[6] examined the electronic states of three-dimensional *trans*-PA with a self-consistent pseudopotential method. They calculated the electron-lattice-displacement coupling constant in the Su-Schrieffer-Heeger[7] (SSH) Hamiltonian and discussed the soliton behavior of *trans*-$(CH)_x$. Recently, Springborg[8] and Ashkenazi *et al.*[9] studied the ground state of PA with a linear muffin-tin-orbitals (LMTO) band-structure approach. Springborg[8] gave an extensive comparison of his results with those of previous calculations. Most recently, von Boehm *et al.*[10] studied the band structure of PA using a self-consistent local-density linear combination of Gaussian orbitals (SCLCGO) approach.

 ©1989 The American Physical Society

In this paper the structural and electronic properties of pristine *trans-* and *cis*-PA are studied from a self-consistent total-energy local-density molecular-cluster approach. This full-potential calculation and the cluster model have an advantage of being able to treat defect carrier states as well as the pristine ground state. (Kink defects and electronic excitations in PA are presented in the following paper.) A brief description of the theory used is given in Sec. II. The basis sets for variational calculations and potential fitting were investigated with ethylene as a prototype. (As illustration, the results on ethylene are discussed and compared with available experimental values in the Appendix.) Results for PA are given in Sec. III. First, we tested the convergence of the energy gap versus the size of the cluster. In addition to direct total-energy calculations, the Slater transition-state approach is used to provide estimates of excitation energies. The energy gap and the positions of main peaks in the DOS are discussed and compared with observed values. Based on total energies calculated for both structures, we compare the binding energies on *trans-* and *cis*-PA and find that *cis*-PA is less binding than *trans*-PA. The optimum geometry of *trans*-PA is obtained by calculating the total energy for varying bond lengths. The total energy for the most stable structure of *trans*-PA is compared (i) with that of the undimerized state to verify Peierls's theory of distortion, and (ii) with the dimerized calculation of SSH.[7] Finally, we discuss the prospects and limitations of the finite-chain model.

II. THEORETICAL APPROACH

The local-density-functional (LDF) molecular-cluster approach as used in these studies employed the discrete variational method (DVM) and an efficient potential-expansion scheme to perform the calculations. This method has been successfully applied to several problems,[11] and since the details of the formalism were presented previously,[12] we only describe some main features here. The Hohenberg-Kohn-Sham LDF approach[13] leads to one-electron equations which are written in atomic units as

$$(-\tfrac{1}{2}\nabla^2+V_{\rm Coul}+V_{\rm xc})\psi_i=\varepsilon_i\psi_i \ . \tag{1}$$

Here, $V_{\rm Coul}$ is the standard Coulomb potential arising from the electrostatic electron-electron and electron-nuclear interactions, and $V_{\rm xc}$ denotes the exchange-correlation potential which we take as the von Barth–Hedin exchange-correlation potential.[14] The wave functions of the cluster are expanded as

$$\psi_i=\sum_j \chi_j(\mathbf{r})C_{ij} \ , \tag{2}$$

where χ_j are symmetrized linear combinations of numerical atom-centered functions. It has been long known that a minimal basis set is usually not accurate enough for covalent bonds, so "pseudoatomic" orbitals were used to ensure greater variational freedom, i.e., we included some ionic orbitals in the variational space in addition to the occupied orbitals of neutral atoms. (In the Appendix, we examine the effect and convergence of the additional basis set.)

Using linear variational theory, we obtain the standard secular equation with matrix elements determined by discrete sampling. The wave functions and eigenvalues were determined using the self-consistent multicenter-multipolar (SCM) representation of the density.[12] The density basis contains the spherical atomic densities in LCAO numerical form and also different sited radial functions with different partial waves. The coefficients of the density expansion were also obtained by a global least-squares fit to the charge density on the variational points grid.

It is shown in the Appendix that the multipolar expansion in orbital angular momentum l is a well-convergent quantity, and that usually $l\leq 2$ can be used for the linear-chain hydrocarbon systems studied here.

III. RESULTS FOR *trans-* AND *cis*-PA

In this work, pristine (defect-free) PA has been studied with a single-chain cluster model. It is known that the distance between adjacent carbon atoms along a chain is ~ 1.4 Å, while the interchain distance is approximately 3.8 Å. This material shows highly anisotropic properties and since weak insulating interchain coupling is usually expected,[15] we neglected it here. Indeed, it will be seen that the intrachain coupling considered here corresponds well to the main features of the electronic structure of PA. It needs to be emphasized that there is some advantage in using a cluster model for low-dimensional structures; the effects of impurities may also be readily investigated since the periodicity required in energy-band treatments is not a problem here.

Both *trans-* and *cis*-PA were examined with an ethylenelike truncation at the terminals as illustrated in Fig. 1. For *trans*-PA, the C—C, C=C, and C—H bond lengths used in the first stage were 1.46, 1.34, and 1.09 Å, respectively. Both the C—C—H bond angle (120°) and the C=C—H bond angle (127.3°) are taken from Ref. 16. Both *trans-* and *cis*-PA clusters maintained a C_{2h} point-group symmetry when the coordinates were adopted as shown in Fig. 1.

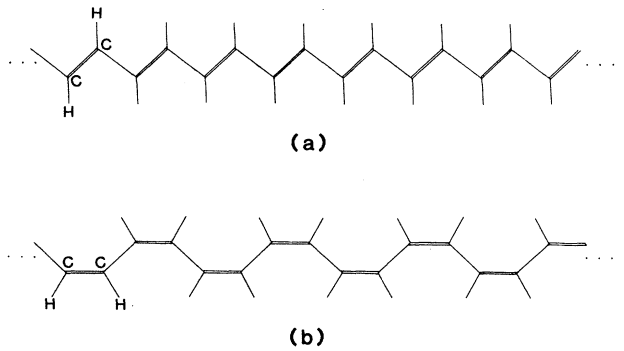

FIG. 1. Schematic geometrical structure of (a) *trans*-polyacetylene and (b) *cis*-polyacetylene.

A. Convergence of the energy gap with the size of the cluster

1. trans-PA

Four clusters of different sizes were investigated: C_8H_{10}, $C_{12}H_{14}$, $C_{16}H_{18}$, and $C_{20}H_{22}$. In Fig. 2 their lowest unoccupied states and the highest occupied states are drawn. For the $C_{20}H_{22}$ cluster, the calculated energy gap of *trans*-PA is 1.68 eV. Since the experimental estimate of the gap from optical-absorption experiments and reflectance spectra[5] is 1.4–1.9 eV, our resulting gap appears to have converged to be in good agreement with the observed value. (Remarkably, it also agrees with the result of an early non-self-consistent band calculation by Grant and Batra.[3])

The convergence with the size of the cluster may also be understood from an eigenvalue–versus–number-order plot, as shown in Fig. 3, for eigenvalues of different symmetry. On the x axis the number order of the eigenvalues was scaled inversely according to the size of the cluster; the y axis showed the corresponding eigenvalues. The slope of the curve described the intensity distribution of the levels. In comparing the four curves it may be seen

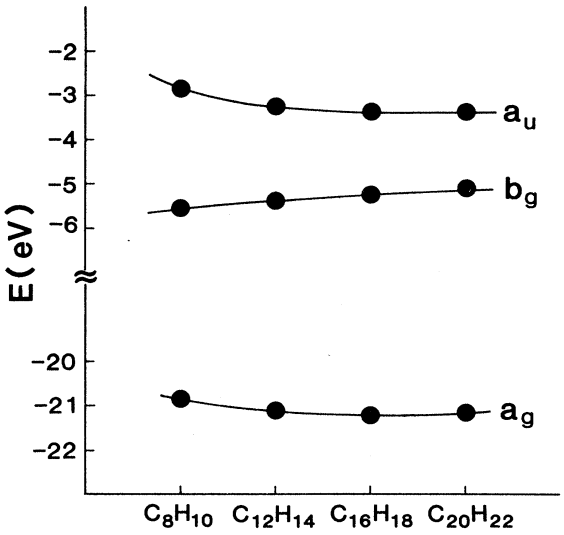

FIG. 2. Plot of the energy gap and valence-band width vs the size of the cluster for *trans*-PA. The lowest unoccupied orbital, the highest occupied orbital, and the lowest valence orbital are a_u, b_g, and a_g, respectively.

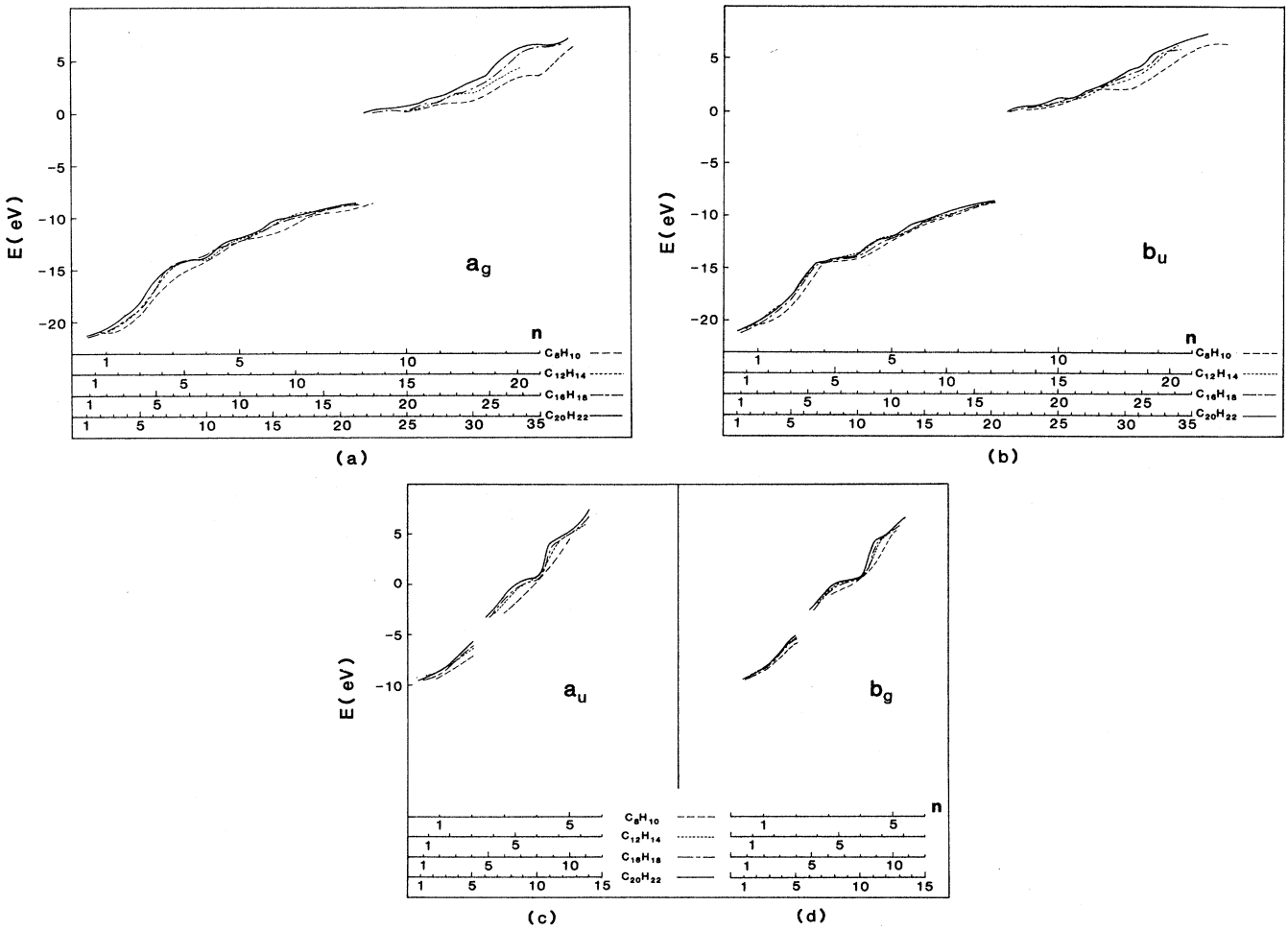

FIG. 3. Plot of eigenvalue vs the orbital index number (energy ordered within one symmetry) for *trans*-PA. The scales on the horizontal axis for different clusters are inversely proportional to the number of carbon atoms in the cluster. The discontinuity of the curves indicates the existence of a gap. (a)–(d) refer to orbitals of different symmetry: (a) a_g, (b) b_u, (c) a_u, and (d) b_g.

that the C_8H_{10} cluster provides too crude a model because it deviates from the three other curves both in value and in shape. By contrast, the three larger clusters are very close in value and shape except in the high-energy region. These curves provide evidence for the convergence of energy levels as a whole. Finally, and most importantly, it may be seen that there is a discontinuous jump in the curve, which implies the existence of a gap in the eigenvalue spectrum.

2. *cis-PA*

Figure 4 shows the convergence of the energy gap for *cis*-PA. It is seen to remain almost flat as the cluster size increases from $C_{16}H_{18}$ to $C_{20}H_{22}$. The energy gap of *cis*-$C_{20}H_{22}$ is 1.74 eV, i.e., slightly larger than that determined for the trans case.

B. Density of states of *trans*-PA and *cis*-PA

The calculated DOS of *trans*-PA is shown in Fig. 5(a). Since a finite-size molecular-cluster model was used, only discrete levels were obtained instead of the continuous band for the infinite structure. Usually, the DOS is obtained by some level-broadening technique, but here we used a nonequidistant histogram to describe the DOS of PA. The density of states was defined here as

$$\mathcal{N}(i)=\frac{1}{N_e(\varepsilon_{i+1}-\varepsilon_i)}\ , \tag{3}$$

where N_e is the number of carbon atoms in the cluster, and ε_i labels the ith eigenvalue. Equation (3) implies that there is one state ranging from ε_i to ε_{i+1}, so the width of each step changes according to the separation between neighboring levels.

From the results in Fig. 5(a), it can be seen that there are two main peaks, A and B, in the valence-band DOS,

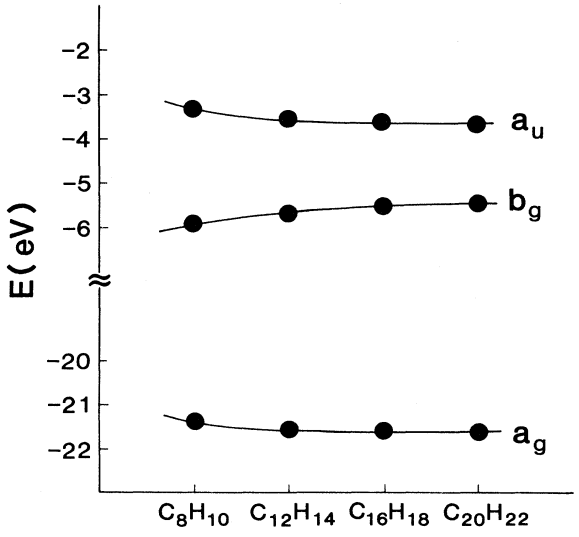

FIG. 4. Plot of the energy gap and valence-band width vs the size of the cluster for *cis*-PA. The lowest unoccupied orbital, the highest occupied orbital, and the lowest valence orbital are a_u, b_g, and a_g, respectively.

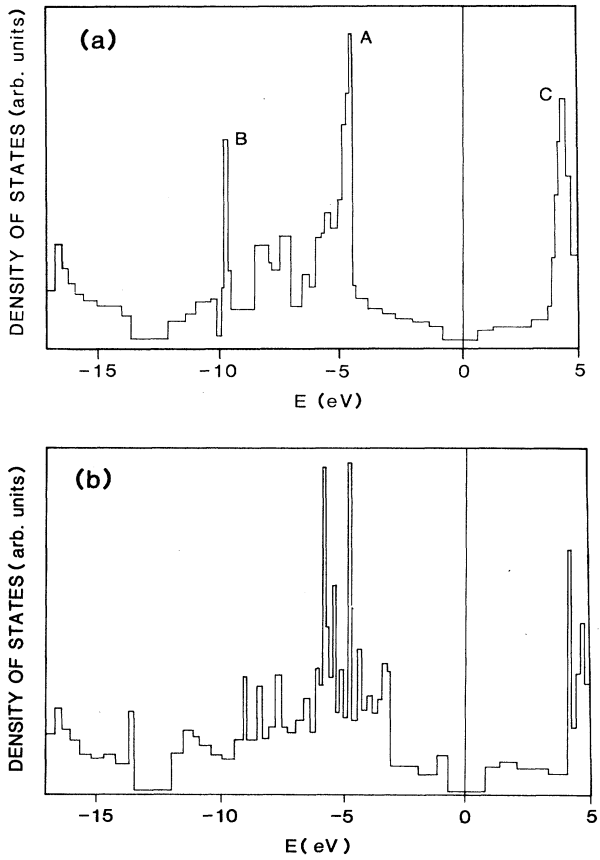

FIG. 5. Density-of-states histogram for (a) a $C_{20}H_{22}$ *trans*-PA cluster and (b) a $C_{20}H_{22}$ *cis*-PA cluster. In both, E_F is labeled as zero energy.

and a peak C in the DOS from the unoccupied band. Comparing calculated results for different cluster sizes, we find that although the details of the histograms deviated from each other the positions of the main peaks were well determined even for the smallest cluster. The positions of these peaks (A, -5.5 eV; B, -9.7 eV; C, 4.0 eV) agree quite well with the experimental x-ray-photoemission-spectroscopy[7] (XPS) results and the theoretical results of Grant and Batra.[3] Peaks A and C arise mainly from the p_x, p_y states of carbon, and are the σ-bonding and antibonding orbitals, respectively. The gap in energy between the σ-bonding and antibonding orbitals is 9.5 eV. This may also be seen from Figs. 3(a) and 3(b), which show the eigenvalue distribution of a_g and b_u symmetry, both of which have carbon σ character. A gap of 9.5 eV is also evident there. Between the σ gap there lie the π-bonding and antibonding states of a_u or b_g symmetry; these arise primarily from the carbon s and p_z contributions and show a lower and rather flat DOS. The gap between the π-bonding and antibonding states was found to be 1.68 eV for *trans*-PA.

The DOS of *cis*-$C_{20}H_{22}$ is shown in Fig. 5(b): different peak structures were found, compared with those obtained for the *trans* case, but the width of the σ-bonding

and antibonding gaps is very close to that of *trans*-PA. Also, the corresponding π-bonding and antibonding gaps do not differ much.

C. Relative stability between *cis*- and *trans*-PA

In comparing the binding energies of *trans*- and *cis*-PA obtained from the calculated total energies for the four different clusters, a 0.1–0.2-eV per C_2H_2 unit lower binding energy was found for the *cis* configuration. These results, listed in Table I, indicate that *trans*-PA is slightly more stable than *cis*-PA. It should be noted that the nonempirical effective Hamiltonian technique for polymers[17] also favored this prediction, whereas previous theoretical studies showed disagreement on this point.[4] Since experimental results[18] have indicated that the *trans* isomer is the thermodynamically stable form at room temperature, calculations which failed to produce the trans form as most stable need reevaluation.

Theoretically, much more attention has been paid to *trans*-PA because of its degenerate ground state, which leads to a prediction of the existence of a topological soliton or kink.[7] *cis*-PA does not have a degenerate ground state: with interchange of single and double bonds, the resulting structure is inequivalent, and so will not have the same energy. However, a kink-antikink defect might also be expected in *cis*-PA as well as in *trans*-PA. These matters are the subject of the following paper.

D. The Peierls distortion and optimum geometry

According to the theory of Peierls,[19] the regular chain structure in a one-dimensional metal with a partly filled band will never be stable, since one can always find a distortion with a suitable value of alternating bond lengths for which a gap will occur at or near the Fermi energy. This results in a reduction of energy due to the separation of bonding and antibonding states.

In this subsection we report a study on the dimerization of *trans*-PA from the total-energy point of view. First, we varied the bond lengths from *trans*-PA around their observed values and the most stable structure was found by minimization of the total energy. Then the undimerized structure was studied. The resulting projected dimerization displacement, u_0, was found to be in good agreement with the experimentally estimated value[20] and with that of SSH.[7] Comparing the total energies of the dimerized and undimerized structures, a reduction of energy was found due to the dimerization, in accordance with Peierls's theory.

In Fig. 6 the total-energy curves for *trans*-PA are given in which (a) the bond length C=C was varied with C—C fixed at its observed value, and (b) the bond length C—C was varied with C=C fixed. The most stable positions given by the minimization of total energy were within 1–1.2% of the experimental values. The total-energy curve for the undimerized chain was also calculated, and the optimum position was found with the bond length 1.39 Å which is the approximate mean value of the single and double bonds of *trans*-PA.

Two main results were obtained from the calculations.

TABLE I. Binding energy of different-size clusters for both *trans*- and *cis*-PA and their binding energy per $(CH)_2$ unit are estimated with respect to the binding energy of ethylene, C_2H_4. *trans*-PA is seen to be slightly more stable than *cis*-PA.

Binding energy (eV)	C_8H_{10}	$C_{12}H_{14}$	$C_{16}H_{18}$	$C_{20}H_{22}$
trans	−85.15	−125.27	−165.78	−206.85
cis	−84.18	−124.19	−164.95	−205.21
Binding energy [eV/$(CH)_2$]				
trans	−20.10	−20.08	−20.13	−20.22
cis	−19.77	−19.87	−20.01	−20.04

First, by comparing the binding energies of the dimerized and undimerized cases, the former was found to be more binding with a difference of 0.02–0.03 eV/(C_2H_2 unit) between the two cases. [Mintmire and White,[21] using the self-consistent LCAO-$X\alpha$ method, found the stabilization energy to be ~0.032 eV/(C_2H_2 unit), which is close to our result.] Thus, the Peierls prediction that dimeriza-

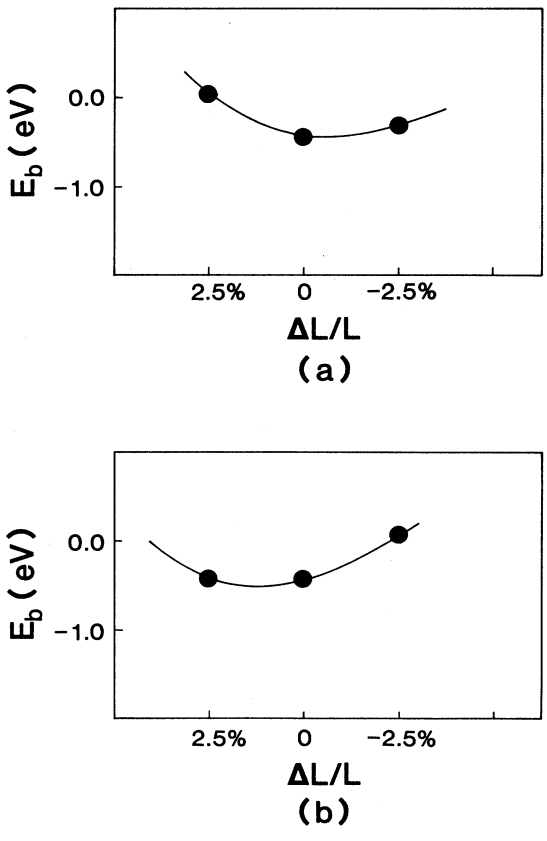

FIG. 6. Total-energy curve for *trans*-PA, $C_{20}H_{22}$. The total binding energy (a) vs the C=C bond length with C—C and C—H fixed, and (b) vs the C—C bond length with C=C and C—H fixed. $\Delta L/L$ on the abcissa indicates the bond-length deviation from the experimental value.

tion brings the chain to a more stable situation with lower total energy is verified quantitatively. The DOS of the undimerized chain was examined and compared with that of dimerized *trans*-PA. It may be seen that the density of states appears to be higher near the Fermi energy Fig. 7 and no valley in the histogram occurred there. A plot of eigenvalues versus number order (not presented) showed smooth continuity across the Fermi energy. All of these data favor an interpretation that no gap exists in the undimerized case and, hence, that it is a metal.

Second, as stated above, the optimum geometry was found to agree well with experimentally estimated values. However, due to the difficulties in preparing single crystals of these quasi-1D semiconducting polymers, it was found[5,21] that important details of their intrachain structure are often not very clear. Hence, the results of these first-principles calculations are of particular value here. From the resulting bond lengths given above, the projected dimerization displacement (along the chain direction) in our calculation was found to be

$$u_0=\frac{1}{\sqrt{3}}\Delta R=\frac{1}{\sqrt{3}}0.060\ \text{Å}=0.035\ \text{Å}\ . \tag{4}$$

This is in good agreement with the x-ray scattering data[20] for *trans*-PA, where the symmetry-breaking dimerization distortion was found to be $u_0\sim 0.03$ Å. The displacement obtained by SSH (Ref. 7) was $u_0\sim 0.04$ Å. Recent work with a LCAO-$X\alpha$ approach[21] gave $u_0\sim 0.02$ Å; however, these authors stated their predicted result might not be very accurate due to the small basis set used.

E. Optical excitation and the band gap

The lowest optical excited state (i.e., $b_g\rightarrow a_u$) of pure *trans*-PA ($C_{16}H_{18}$) and its corresponding Slater transition state[22] were studied in the same way as described for ethylene in the Appendix. The total-energy difference of the excited and ground states (ES) and (GS) is

$$\Delta E(b_g\rightarrow a_u)=E_{\text{tot}}^{\text{ES}}-E_{\text{tot}}^{\text{GS}}=1.90\ \text{eV}\ .$$

Note that this value is at the high end of the experimental gap values.[5] As expected, it is also higher than the gap obtained from the LDF ground-state eigenvalues, which are well known to underestimate excited-state properties like band gaps.

In the self-consistent Slater transition-state (TS) calculation, half an electron was taken away from the highest occupied b_g level and put into the lowest unoccupied a_u level. The difference of the eigenvalues between these two levels is

$$\Delta E^{\text{TS}}=E_{a_u}^{\text{TS}}-E_{b_g}^{\text{TS}}=1.88\ \text{eV}\ .$$

Thus, there is only a discrepancy of 0.02 eV from the total-energy result, indicating that the quasiparticle transition-state method gives a reliable estimate of electronic excitations here, as in many other systems. This fact will simplify future studies of excitation features such as those studied in the following paper.

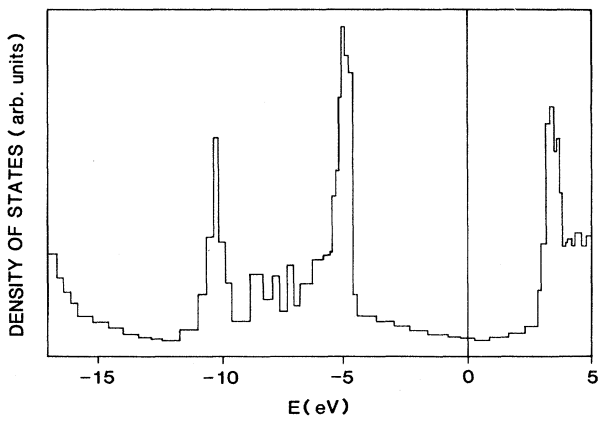

FIG. 7. Density-of-states histogram for an undimerized $C_{20}H_{22}$ *trans*-PA.

IV. CONCLUSIONS

We have studied the structural, electronic, and optical properties of *trans*- and *cis*-polyacetylene using a precise local-density, total-energy, molecular-cluster approach. The use of extended basis sets in a LCAO representation and the use of accurate multipolar potential representations was found to be important in obtaining reliable results. Calculations on ethelene (C_2H_4) given in the Appendix verified the accuracy of both the total-energy and transition-state approaches to cohesive and excitation energies.

Chain clusters C_nH_{n+2} with $n=8,12,16,20$ were studied, and good convergence of densities of states, energy gaps, and other measures of the electronic structure was observed. Variations of molecular conformation around the equilibrium geometry were carried out to explore structural stability. *trans*-PA was found to be slightly more stable (by ≤ 0.02 eV per C_2H_2 unit) than the *cis* form, in agreement with experiment. The dimerization energy accompanying the Peierls's distortion was calculated to be 0.02–0.03 eV per C_2H_2 unit—which is somewhat larger than previous estimates. The calculated projected dimerization displacement (0.035 Å) was found to be in very good agreement with x-ray data (~ 0.03 Å).

These results demonstrate that relatively small finite-chain models provide quantitatively accurate representations of quasi-one-dimensional molecular crystals of current interest. In the following article we present an analysis of kink and kink-antikink defect structures which are of great importance in describing the transport properties of materials like polyacetylene.

ACKNOWLEDGMENTS

This work was supported in part by the U.S. National Science Foundation [through the Northwestern University Materials Research Center (Grant No. DMR-88-21571) and by a grant from its Division of Advanced Scientific Computing at the National Center for Supercomputer Applications at the University of Illinois at Urbana-Champaign], by the U.S. Department of Energy (Grant No. DE-FG02-86-56097A01), and by a computing grant from Cray Research, Inc.

TABLE II. Basis-set effects on binding energy in ethylene. The experimental geometry was used throughout: R(C—C)=2.5304 a.u., R(C—H)=2.0505 a.u., <H—C—H=117.83°. All results refer to self-consistent-field (SCF) ground-state calculations, using the von Barth–Hedin exchange-correlation potential, and partial waves $l \leq 2$ in the density expansion. Binding energies are calculated with respect to spin-polarized free atoms with the same LD-potential scheme.

	Basis 1	Basis 2	Basis 3	Basis 4	Basis 5	Basis 6
Basis	$C^0_{1s2s\,2p}$	$C^0_{1s2s\,2p}$ $C^{1+}_{2s\,2p}$	$C^0_{1s2s\,2p}$ $C^{2+}_{2s\,2p}$	$C^0_{1s2s\,2p}$ $C^{1+}_{2s\,2p}$ O^{7+}_{3d}	$C^0_{1s2s\,2p}$ $C^{2+}_{2s\,2p}$ O^{7+}_{3d}	$C^0_{1s2s\,2p}$ $C^{1+}_{2s\,2p}$ O^{7+}_{3d4f}
	H^0_{1s}	H^0_{1s} $H^{0.5+}_{1s}$	H^0_{1s} $H^{0.5+}_{1s}$	H^0_{1s} $H^{0.5+}_{1s}$	H^0_{1s} $H^{0.5+}_{1s}$	H^0_{1s} $H^{0.5+}_{1s}$
Binding energy (eV)	−17.49	−24.85	−24.91	−25.32	−25.37	−25.32

APPENDIX: THE SELECTION OF BASIS SET AND POTENTIAL FITTING: C_2H_4

It is desirable to choose an adequate basis set for the wave functions of the cluster. We have attempted to "optimize" a basis by making reference calculations on a small hydrocarbon molecule. We used ethylene, C_2H_4, as a prototype since we end the finite PA chain with an ethylenelike truncation and need to find a good basis set for carbon and hydrogen to be used in all subsequent chain calculations. In addition to the $1s,2s,2p$ states of the neutral carbon atom and the $1s$ state of the neutral hydrogen atom, we also adopted some atomic orbitals of ionic carbon and hydrogen or those of some highly ionized heavier ions like oxygen. These ionic basis functions are well adopted to describe short-range details of the reshaping of valence molecular orbitals (MO's) in the interatomic regions. The results are listed in Table II. When a minimal basis set of neutral atoms was employed, the total energy showed insufficient binding. The $2s,2p$ orbitals of C^{n+} ($n=1,2,3,\ldots$) did bring an essential improvement to the basis, while the $3d$ (or $4f,\ldots$) orbitals of O^{7+} gave only a small contribution.

As described in Sec. II, the charge density was expanded in a multicenter overlapping multipolar form. The convergence of the energy with partial wave l, listed in Table III, shows good convergence with l when $l=0,1,2$; the eigenvalues in the self-consistent calculation also converged well for $l \geq 1$ and the C^{n+} basis. In the last two or three iterations out of 15 interations, the error in the location of the Fermi energy is usually less than 0.01 eV.

The calculations for ethylene were done in two stages. First, we used the C=C and C—H bond lengths of 2.5304 and 2.0505 a.u.; the H—C—H bond angle was adopted as[23] 117.83°. The symmetry of this molecule is D_{2h} (see Fig. 8). Our calculated ethylene binding energy, −0.932 a.u., compares very well with the experimental value of −0.994 a.u.,[24] while the previous theoretical results in the Hartree-Fock approximation lie around −0.648 a.u. (Ref. 25) to −0.696 a.u. (Ref. 26).

The lowest optical excitation state was calculated with one electron moved from the highest occupied state b_{2u} to the lowest unoccupied state b_{3g}. The total-energy difference between this excited state and the ground state is

$$\Delta E(b_{2u}\rightarrow b_{3g})=E^{\rm ES}_{\rm tot}-E^{\rm GS}_{\rm tot}=E^{\rm ES}_{\rm bind}-E^{\rm GS}_{\rm bind}=5.84\ \text{eV}\ .$$

The corresponding Slater transition state[22] was studied with half an electron moved from the highest occupied b_{2u} level to the lowest unoccupied b_{3g} level. The difference of eigenvalues between these two levels is

$$\Delta E^{\rm TS}=\varepsilon^{\rm TS}_{b_{3g}}-\varepsilon^{\rm TS}_{b_{2u}}=5.86\ \text{eV}\ .$$

Note that $\Delta E(b_{2u}\rightarrow b_{3g})$ and $\Delta\varepsilon^{\rm TS}$ differ by only 0.02 eV, which shows good consistency of the theory in calculating ground and excited states by this approach. Now, the absorption spectrum of ethylene[27] shows that the longest-wavelength absorption is a progression of extremely weak and diffused bands from 3400 Å (~2.65 eV), which are singlet-triplet transitions, i.e., spin-forbidden transitions that we have not taken into consideration in our spin-restricted calculation. A much stronger adsorption begins from 2100 Å (~5.91 eV). Our calculated result on optical excitation (5.84–5.86 eV) is in very good agreement with this experimental result.

TABLE III. Convergence of binding energy with improvements in potential expansion for C_2H_4.

	Potential fit, l=				
	0	1	1	1	2
Basis[a]	4	4	2	3	5
Binding energy (eV)	−24.80	−25.22	−24.82	−24.86	−25.37

[a]See Table II.

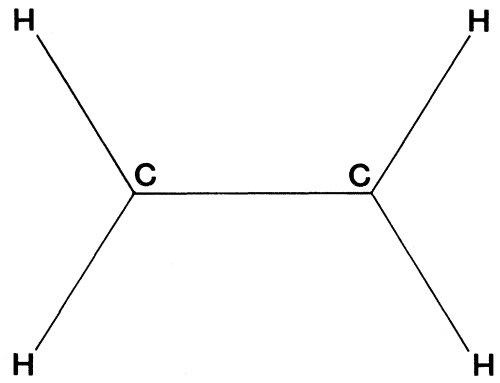

FIG. 8. Schematic bond structure of ethylene.

Further, the ionization state (IS) with one electron taken away from the highest occupied level is compared with the ground state, which gives

$$\Delta E_{\mathrm{IP}} = E^{\mathrm{IS}}_{\mathrm{tot}} - E^{\mathrm{GS}}_{\mathrm{tot}} = E^{\mathrm{IS}}_{\mathrm{bind}} - E^{\mathrm{GS}}_{\mathrm{bind}} = 11.83 \text{ eV} .$$

The eigenvalue of the highest occupied level in the corresponding transition-state calculation (with half an electron taken away from the highest occupied level) is $\varepsilon^{\mathrm{TS}}_{B_{2u}} = -11.66$ eV. In this case, the agreement with the total-energy results is only within <0.2 eV, indicating—as found previously—that the transition-state approach for ionization energies is not as reliable as it is for excitation energies. Further evidence for this is seen from the fact that, while the photoelectron spectrum of ethylene[28] shows that the first adiabatic ionization potential is 10.51 eV, our calculated results (11.66–11.83 eV) differ by over 1 eV.

Finally, in the second stage of our calculations, the bond lengths were varied around their experimental values and the optimum geometry was obtained by minimization of the total energy. First, the total energy around the equilibrium value of the C=C bond length was determined with the bond angles and the C—H bond length fixed at their experimental values. The most stable position was found to be in good agreement with the observed value. Next, the C—H bond length, determined in a similar way. In both, the agreement with their observed values were found to be within 1%.

The basis set and potential-fitting scheme used for ethylene were adopted in the calculations on PA, where we used an ethylenelike terminal group to truncate the PA chain. Since good agreement was found for the ethylene results compared with experimental binding energy and geometry, we believe that this is an accurate approach.

[1]S. Etemad, A. J. Heeger, and A. G. MacDiarmid, Annu. Rev. Phys. Chem. **33**, 443 (1982); W. P. Su, J. R. Schrieffer, and A. J. Heeger, Phys. Rev. Lett. **42**, 1698 (1979); M. J. Rice, Phys. Lett. **71A**, 152 (1979); H. Takayama, Y. R. Lin-Liu, and K. Maki, Phys. Rev. B **21**, 2388 (1980); in Proceedings of the International Conference on Low Dimensional Conductors, edited by A. J. Epstein and E. M. Conwell [Mol. Cryst. Liq. Cryst. **77** (1981) and **83** (1982)].

[2]A. J. Heeger, D. Moses, and M. Sinclair, Synth. Met. **15**, 95 (1986); F. Kajzar, S. Etemad, G. L. Baker, and J. Messier, *ibid.* **17**, 563 (1987).

[3]P. M. Grant and I. P. Batra, Solid State Commun. **29**, 225 (1979).

[4]A. Karpfen and R. Holler, Solid State Commun. **37**, 179 (1981).

[5]R. V. Kasowski, E. Caruthers, and W. Y. Hsu, Phys. Rev. Lett. **44**, 676 (1980).

[6]P. M. Grant and I. P. Batra (unpublished).

[7]W. P. Su, J. R. Schrieffer, and A. J. Heeger, Phys. Rev. B **22**, 2099 (1980); **28**, 1138(E) (1983).

[8]M. Springborg, Phys. Rev. B **33**, 8475 (1986); M. Springborg and O. K. Andersen (unpublished).

[9]J. Ashkenazi, E. Ehrenfreund, Z. Vardeng, and O. Brafman, Mol. Cryst. Liq. Cryst. **117**, 193 (1985).

[10]J. von Boehm, P. Kuivalainen, and J. L. Calais, Phys. Rev. B **35**, 8177 (1987).

[11]B. Delley, D. E. Ellis, A. J. Freeman, E. J. Baerends, and D. Post, Phys. Rev. B **27**, 2132 (1983); S. J. Chou, A. J. Freeman, S. Grigoras, T. M. Gentle, B. Delley, and E. Wimmer, J. Am. Chem. Soc. **109**, 1880 (1987).

[12]B. Delley and D. E. Ellis, J. Chem. Phys. **76**, 1949 (1982); B. Delley, A. J. Freeman, and D. E. Ellis, Phys. Rev. Lett. **50**, 488 (1983).

[13]P. Hohenberg and W. Kohn, Phys. Rev. **136**, B864 (1964); W. Kohn and L. Sham, *ibid.* **140**, A1133 (1965).

[14]U. von Barth and L. Hedin, J. Phys. C **5**, 1629 (1972).

[15]C. R. Fincher, Jr., D. L. Peebles, A. J. Heeger, M. A. Druy, Y. Matsumura, A. G. MacDiarmid, H. Shirakawa, and S. Ikeda, Solid State Commun. **27**, 489 (1978).

[16]R. H. Baughman, S. L. Hsu, G. P. Pez, and A. J. Signorelli, J. Chem. Phys. **68**, 5405 (1978).

[17]J. I. Brédas, R. R. Chance, R. Silbey, G. Nicolas, and Ph. Durand, J. Chem. Phys. **75**, 255 (1981).

[18]C. K. Chiang, C. R. Fincher, Jr., Y. W. Park, A. J. Heeger, H. Shirakawa, E. J. Louis, S. C. Gau, and A. G. MacDiarmid, Phys. Rev. Lett. **39**, 1098 (1977).

[19]R. E. Peierls, *Quantum Theory of Solids,* 1st ed. (Oxford University Press, Oxford, 1955), p. 108.

[20]C. R. Fincher, Jr., C. E. Chen, A. J. Heeger, A. G. MacDiarmid, and J. B. Hastings, Phys. Rev. **48**, 100 (1982).

[21]J. W. Mintmire and T. C. White, Phys. Rev. Lett. **50**, 101 (1983).

[22]J. C. Slater, *Quantum Theory of Molecules and Solids* (McGraw-Hill, New York, 1974), Vol. 4.

[23]*Landolt-Börnstein, New Series II/7, Structure Data of Free Polyatomic Molecules,* edited by K. H. Hellwege (Springer-Verlag, New York, 1976), p. 179.

[24]C. Hollister and O. Sinanoglu, J. Am. Chem. Soc. **88**, 13 (1966).

[25]J. M. Schulman, J. W. Moskowitz, and C. Hollister, J. Chem. Phys. **46**, 2759 (1967).

[26]R. Ahlrichs, H. Lishka, B. Zuraski, and W. Kutzelnigg, J. Chem. Phys. **63**, 4685 (1975).

[27]G. Herzberg, *Molecular Spectra and Molecular Structure* (Van Nostrand, New York, 1966), Vol. III, p. 533.

[28]D. W. Turner, C. Baker, A. D. Baker, and C. R. Brundle, *Molecular Photoelectron Spectroscopy* (Wiley-Interscience, New York, 1970), p. 166.